PCCP

A microfluidic platform for quantitative measurements of effective protein charges and single ion binding in solution

Journal:	*Physical Chemistry Chemical Physics*
Manuscript ID:	CP-ART-02-2015-000746.R1
Article Type:	Paper
Date Submitted by the Author:	23-Mar-2015

Complete List of Authors:	Herling, Therese; University of Cambridge, Department of Chemistry Arosio, Paolo; University of Cambridge, Department of Chemistry Müller, Thomas; University of Cambridge, Department of Chemistry Linse, Sara; Lund University, Biochemistry Knowles, Tuomas; University of Cambridge, Department of Chemistry

Physical Chemistry Chemical Physics
CREATED USING THE RSC LaTeX PCCP ARTICLE TEMPLATE – SEE www.rsc.org/electronicfiles FOR DETAILS
ARTICLE TYPE www. rsc.org/xxxxxx | XXXXXXXX

A microfluidic platform for quantitative measurements of effective protein charges and single ion binding in solution

Therese W. Herling,[a] Paolo Arosio,[a] Thomas Müller,[a] Sara Linse,[b‡] and Tuomas P. J. Knowles[a‡]

Received Xth XXXXXXXXXX 20XX, Accepted Xth XXXXXXXXX 20XX
First published on the web Xth XXXXXXXXXX 200X
DOI: 10.1039/b000000x

The charge state of proteins in solution is a key biophysical parameter that modulates both long and short range macromolecular interactions. However, unlike in the case of many small molecules, the effective charges of complex biomolecules in solution cannot in general be predicted reliably from their chemical structures alone. Here we present an approach for quantifying the effective charges of solvated biomolecules from independent measurements of their electrophoretic mobilities and diffusion coefficients in free solution within a microfluidic device. We illustrate the potential of this approach by determining the effective charges of a charge-ladder family of mutants of the calcium binding protein calbindin D_{9k} in solution under native conditions. Furthermore, we explore ion-binding under native conditions, and demonstrate the ability to detect the chelation of a single calcium ion through the change that ion binding imparts on the effective charge of calbindin D_{9k}. Our findings highlight the difference between the dry sequence charge and effective charge of proteins in solution, and open up the route towards rapid and quantitative charge measurements in small volumes in the condensed phase.

1 Introduction

Electrostatic interactions play a central role in many facets of protein behaviour, including in the context of non-covalent protein-ligand binding [1] that underlies signalling pathways in nature. The charge state of proteins in solution is therefore integral to their function, but commonly remains challenging to quantify experimentally or predict theoretically. The electrostatic characteristics of polyelectrolytes such as proteins are significantly more complex than those of small molecules due to factors including pK_a perturbation of charged moieties and charge screening either by solvent molecules or by the polypeptide chain itself. Thus, the effective charges of solvated proteins are challenging to predict and model accurately. [1–3] Due to their importance for protein function, a considerable effort has been focused on the development of computational tools for the determination of the charge and tautomerisation states of functional groups in native proteins. In some studies, good agreement has been observed between theory and experiment. [4–7]

In addition to non-specific screening, specific chemical interactions between proteins and ions in solution can modify their overall charges. [8] The characterisation of protein-ligand binding represents a complex challenge, which has been addressed through both experiments and theory. [4,9–11] In recent years, protein-ligand binding has been approached from a quantum mechanical perspective aiming to provide detailed information of the free energy of ligand binding and the optimum conformation of the protein-ligand complex. [9–11]

The ability to obtain experimental insights into the effective charges of macromolecules in solution is therefore crucial for the accurate evaluation of the electrostatic environment of a protein under a given set of solution conditions. Movement of proteins in an applied electric field is often used to gain insight into their charge states through evaluation of their respective electrophoretic mobilities. [12–21] The electrophoretic mobility, μ_e, of molecules in solution is determined by their effective charge, q, and diffusion coefficient, D. This parameter is thus a key observable in studies of the effective charge states of proteins. The electrophoretic mobility of proteins in solution has been investigated through measurements of the relative migration in an electric field or the zeta potential, ζ, using approaches such as capillary electrophoresis, native gel electrophoresis, free-flow electrophoresis, and light scattering. [12–21]

With the aims of investigating the effective charge of a protein as a function of the dry charge as predicted from the amino acid sequence and to quantify the effect of specific ion binding, we focused on calbindin D_{9k}. Calbindin D_{9k} is a cytosolic calcium binding protein, here we have studied the bovine minor A form. [23] The 75 amino acid protein contains two EF-

† Electronic Supplementary Information (ESI) available: [details of any supplementary information available should be included here]. See DOI: 10.1039/b000000x/

[a] *Department of Chemistry, University of Cambridge, Cambridge, UK.*
[b] *Department of Biochemistry and Structural Biology, Lund University, Lund, Sweden*
‡ To whom correspondence should be addressed: Sara.Linse@biochemistry.lu.se and tpjk2@cam.ac.uk.

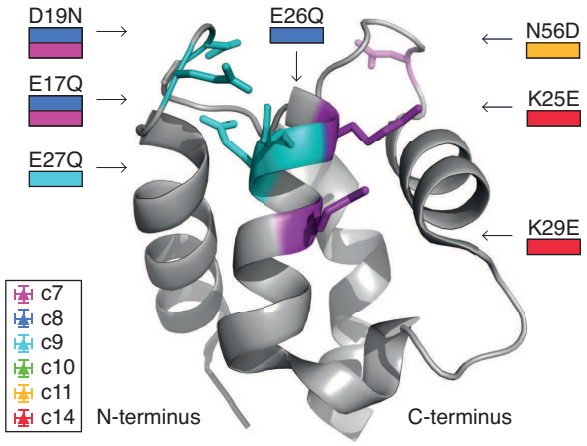

Fig. 1 Calbindin D_{9k}. Crystal structure of calbindin D_{9k} with the two Ca^{2+} binding loops at the top of the structure (PDB 4ICB).[22] The protein charge ladder constructs were named according to their predicted negative sequence charge: c7 - c14. Here the mutated charged residues are highlighted: cyan for the removal of a negative charge, pink for the introduction of a negative charge, and purple for the replacement of a positive charge with a negatively charged residue. The constructs in which a given substitution is present are shown by the coloured bars below the label.

hand motifs,[24] which can each chelate one Ca^{2+} ion.[22,25,26] Variation in the intracellular Ca^{2+} concentration plays a crucial role in a number of vital cellular signalling pathways, controlling for instance memory and learning as well as cell death through apoptosis. Calbindin D_{9k} acts as a Ca^{2+} buffer and facilitates calcium uptake in the gut by transporting Ca^{2+} across the cytosol of enterocytes.[27] The positive cooperativity of Ca^{2+} binding by the two EF-hands is key to the function of calbindin D_{9k}.[26] The three-dimensional structure of calbindin is well characterised both by nuclear magnetic resonance spectrometry, NMR, and X-ray crystallography.[22,25,28,29] The protein is highly stable towards denaturation[30] and the individual pK_a values have been measured for its 27 ionizable sidechains.[31–33] This protein thus represents an ideal system for our studies.

Here we show that by combining microfluidic measurements of the sample electrophoretic mobility and diffusion coefficient we have developed a robust approach for determining the effective charge of solvated proteins experimentally. Furthermore, we have demonstrated the applicability of this technique to probe non-covalent interactions. In the present study we quantified the change in net charge upon ion coordination and were able to detect the specific binding of calbindin D_{9k} to a single calcium ion.

2 Results

A microfluidic platform for the determination of effective protein charges

In order to develop a platform for the convenient and quantitative determination of protein charges in solution, we have combined measurements of the diffusion coefficient and the mobility of the molecule under the action of an external field within a microfluidic device. These two quantities can be coupled through the fluctuation-dissipation theorem to the effective charge of the protein. In particular, the drag that defines the motion of a particle in a field is determined by the same quantity, the diffusion coefficient D, that governs the fluctuations of a particle under Brownian motion. This relationship is described for a spherical particle by the Stokes-Einstein equation:

$$D = \frac{k_B T}{6\pi\eta R_H}, \quad (1)$$

For a sphere D is determined by the viscosity of the solution, η, and the hydrodynamic radius, R_H, where k_B and T are the Boltzmann constant and absolute temperature, respectively.[34] The electrophoretic mobility of a species in solution is by dimensionality arguments related to D and a charge component, the effective charge q.[34] This connection is described by the Nernst-Einstein relation:

$$\mu_e = \frac{qD}{k_B T}, \quad (2)$$

The value of μ_e can furthermore be related to the zeta potential, ζ, via the Hückel equation†. This fluctuation-dissipation relationship has been used as the basis for determining the ζ-potential from light scattering measurements.[34] We used the simple and well-defined relationship in equation 2 to obtain an absolute measure of the effective charges of the calbindin constructs in solution. A particular feature of this approach is that it enables the effective charge to be determined without the need to make any assumptions regarding the shape of the analyte. We achieved this objective through the application of a microfluidic technique to measure D and the direct use of this value in equation 2.

For the measurement of the mobility of solvated proteins in an electric field, we used micro free-flow electrophoresis. Macro scale free flow electrophoresis was introduced several decades ago,[12] and recent progress in microfabrication methods has allowed a number of approaches to be developed for the integration of electrodes within microfluidic devices[35–43] in order to perform micro-free flow electrophoresis that does not require large sample volumes or, in some cases, high voltages.

Here, we have used soft lithography methods to achieve the integration and automatic alignment of 3 dimensional electrodes in direct contact with microfluidic channels

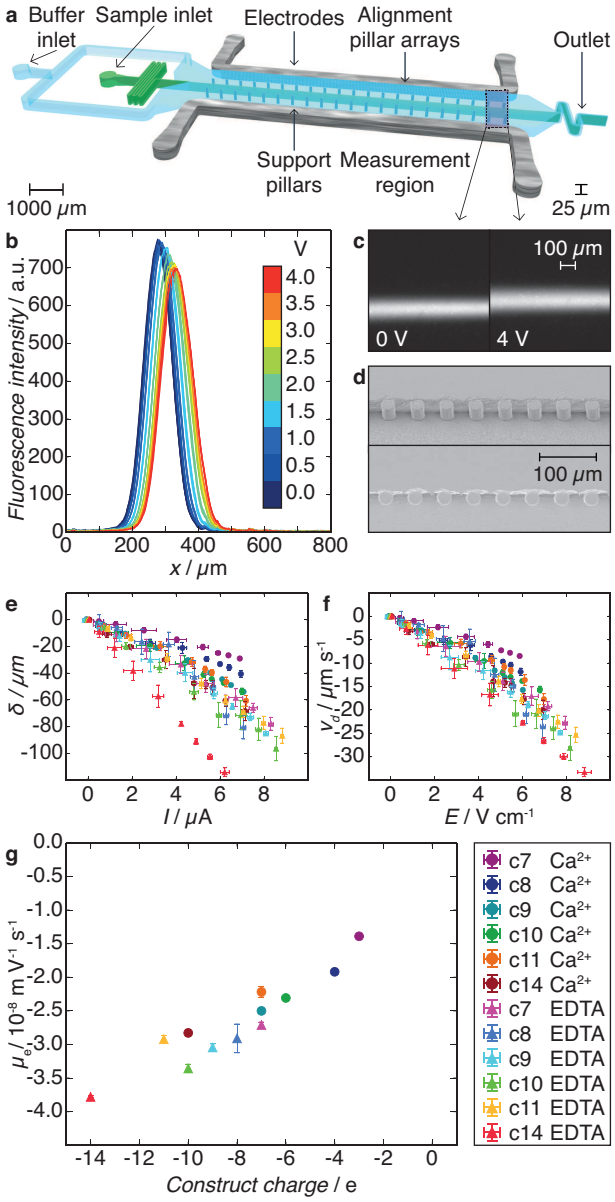

Fig. 2 Microfluidic free-flow electrophoresis. (a) Diagram of the microfluidic device design. Microsolidic components are shaded in grey.[43] The main channel contains pillar arrays for positioning of the solder and support of the channel ceiling. (b) Fluorescence intensity profiles of c9 in Ca^{2+}, showing four repeats of a voltage ramp from 0 - 4 V in blue - red. (c) Fluorescence images of analyte, c9 in Ca^{2+}, at 0 V and 4 V. (d) SEM images of the electrodes aligned by a micro-pillar array. Top: the electrode interface at an angle. Bottom: the electrodes as seen from the camera. (e) The measured sample deflections and currents at each applied potential for the six construct in the presence of Ca^{2+} or EDTA, error bars show the standard deviation for four repeats. (f) Electrophoretic velocity of the analytes against electric field, the slope gives the electrophoretic mobility. (g) The electrophoretic mobilities plotted against the predicted charge at pH 8.0, the error bars represent the error on the linear fit to (f). The legend applies to panels (e - g).

as described in the electronic supplementary information, ESI†.[41,43] The integration of solid wall electrodes flanking microfluidic channels allowed a uniform electric field to be applied across aqueous solutions. Moreover, calibration of the cell constant and buffer conductivity allowed determination of the electric field experienced by analyte molecules during the experiment†. From these measurements the electrophoretic mobility of proteins in solution could be quantified. The resulting absolute values for μ_e permitted findings to be compared between multiple buffer systems at a range of different concentrations.[43] Quantitative free-flow electrophoresis could thus be applied to determine the electrophoretic mobility of solvated macromolecules directly, without the need for reference molecules as mobility standards.

A charge ladder of calbindin D_{9k} constructs

We studied six calbindin D_{9k} constructs with point mutations conferring a range of predicted naked charges.[44–46] In order to visualise these constructs in the electrophoresis experiments AlexaFluor488 was conjugated to a lysine residue as described in Experimental procedures, thereby removing one positive charge. The dye itself has a predicted net charge of - 2 e.[47] Thus the addition of a fluorescent probe decreased the predicted construct sequence charges to between -14 and -7 e, Fig. 1. These calbindin D_{9k} constructs were named according to their predicted negative charge at pH 8.0: c7 - c14. The specific residue changes for each construct are shown in Fig. 1. We introduced variations from the wild-type charge of -10 e by conservative mutations exchanging aspartate and glutamate residues for asparagine and glutamine residues.

Five of the constructs (c7, c8, c10, c11 and c14) contained two functional EF-hand sites. the wild-type minor A form of calbindin D_{9k} has a very high affinity for Ca^{2+} with an average K_d of 3 nM at low ionic strength, as used in the present study.[26] In the constructs c8 and c7 two and three negative surface charges were substituted respectively, these changes have been observed to lead to increased stability and reduced Ca^{2+} affinity with average K_D of 56 nM (c8) and 180 nM (c7).[44,48] The C-terminal EF-hand of calbindin D_{9k} contains an Asn-Gly sequence at residues 56-57, which is sensitive to deamidation. In the c11 construct, N56 was replaced with D56, thus representing the deamidated α-isoform with largely retained Ca^{2+} affinity.[46] In construct c14, two lysine residues on the protein surface were replaced with glutamate residues leading to a nominal change in the surface charge of -4 e. The very high similarity of the NMR spectrum of this variant to that of the wild-type indicate none or only very local structural changes.[45] One of the constructs, c9, contained the point mutation E27Q, Fig. 1. This glutamate residue serves as a bidentate ligand providing two oxygens for Ca^{2+} coordination, the mutation was therefore expected to disrupt calcium

ion chelation by the N-terminal EF-hand, as found upon E to Q mutations at this position in other EF-hands.[49] Thus, in the presence of 0.1 mM Ca^{2+} c9 would only be expected to bind a single calcium ion, while the other five constructs would be expected to bind two. In addition, we were able to modulate the predicted construct charges through the addition of either calcium ions or a large excess of the chelating agent ethylenediaminetetraacetic acid, EDTA, thereby creating a charge ladder of protein constructs with predicted charges ranging from -14 to -3 e. These charge ladder proteins were recombinantly expressed, purified and labelled with Alexa488 as described in the ESI†and previously reported.[26,50,51]

Microfluidic free-flow electrophoresis

Microfluidic free-flow electrophoresis experiments were performed for each of the six constructs in 5 mM Tris-HCl buffer pH 8.0 containing either 0.1 mM EDTA or 0.1 mM $CaCl_2$, Fig. 2. In this manner, we were able to measure the electrophoretic mobility of both the apo- and the calcium bound form of calbindin. Within the microfluidic device, the sample stream was flanked by buffer between integrated InBiSn electrodes, Fig. 2(a+d). Sample molecules migrated according to their electrophoretic mobility perpendicularly to the direction of flow upon the application of an electrical potential between the electrodes. The position of the sample signal was recorded for applied potentials of 0 - 4 V at 0.5 V intervals, Fig. 2(b) shows the sample fluorescence intensity for a cross section of the channel for four repeats of the voltage ramp. The deflection, δ, and current, I, were measured as a function of the applied voltage, V, for each of the 12 samples, shown in Fig. 2(e).

The cell constant characterising each set of electrodes was determined by measurements of the conductance of a KCl solution of known conductivity as described in the ESI†.[43] The conductivities, σ, of the buffer solutions used were then determined from measurements of their conductance in the electrophoretic devices. Through these measurements we were also able to take into account variation between individual microfluidic devices and buffer solutions used, Fig. 2(e) and (f).

Combining the buffer conductance in a given device and the measured current and using Ohm's law we determined the effective voltage drop, $V_{\text{effective}}$, across the solution. We were then able to obtain an absolute value for the electric field strength, E, across the solution from division of $V_{\text{effective}}$ by the distance between the electrodes. The electrophoretic velocities, v_d, were calculated by division of δ by the residence time between the electrodes, which was known from the flow rate through the device and the channel dimensions, Fig. 2(f). Linear fits to the slopes of the plots of velocity against electric field, shown in Fig. 2(f), were then performed to determine the electrophoretic mobility, $\mu_e = v_d/E$, of each construct, Fig. 2(g)[43].

Measurements of the charge ladder diffusion coefficients

The diffusion coefficient of proteins in solution can be evaluated through observation of their diffusion perpendicularly to the direction of flow under laminar flow conditions within microfluidic channels.[52–55] We performed microfluidic diffusion experiments to measure the diffusion coefficients of each construct in both of the buffer solutions used, Fig. 3. For each construct we recorded the fluorescence intensity profile of the analyte diffusing into flanking buffer solution at 12 time points within the channel shown in Fig. 3(a) at three different flow rates, Fig. 3(b). For each data set the diffusion coefficient best describing the observed fluorescence profiles was determined through a least squares fit of simulated diffusion profiles to the data†, Fig. 3(c).[55] These experiments enabled us to probe for changes in the construct size due to the point mutations, but also to investigate whether the addition of the fluorescent label had altered the size of calbindin markedly.

We found that the diffusion coefficient of calbindin did not vary considerably between constructs and solution conditions. This is in agreement with previous studies indicating that the binding of Ca^{2+} does not lead to extensive structural changes in of the protein calbindin D_{9k}.[29] We then used the measured diffusion coefficients to estimate the size of the calbindin constructs. The relation between the diffusion coefficient and dimensions describing proteins and their complexes can be challenging to describe for non-globular conformations.[56] However, structural studies have found calbindin D_{9k} to be a globular protein.[22,29] From the measured diffusion coefficients we therefore calculated the corresponding hydrodynamic radii, R_h, assuming a spherical shape and using the Stokes-Einstein equation. We found the mean radius to be 1.5 ± 0.2 nm, which is in good agreement with previously reported values, Fig. 3(c).[22,29] These results also indicate that the attachment of AlexaFluor488 did not change the size of the protein significantly.

Effective charges of the charge ladder constructs in solution

The effective charges of the calbindin constructs were calculated through the use of the measured electrophoretic mobilities and the diffusion coefficient. We note, that here the value for the diffusion coefficient was used directly, without assuming a specific shape or the corresponding hydrodynamic radius. The microfluidic experiments were performed at pH 8.0, which is outside the previously reported range of pK_a values for the acidic residues[32]. Experimentally determined values pK_a for the carboxylic side-chains have been reported, with the highest being 6.5 for Glu27.[32] At pH 8.0 primary amine

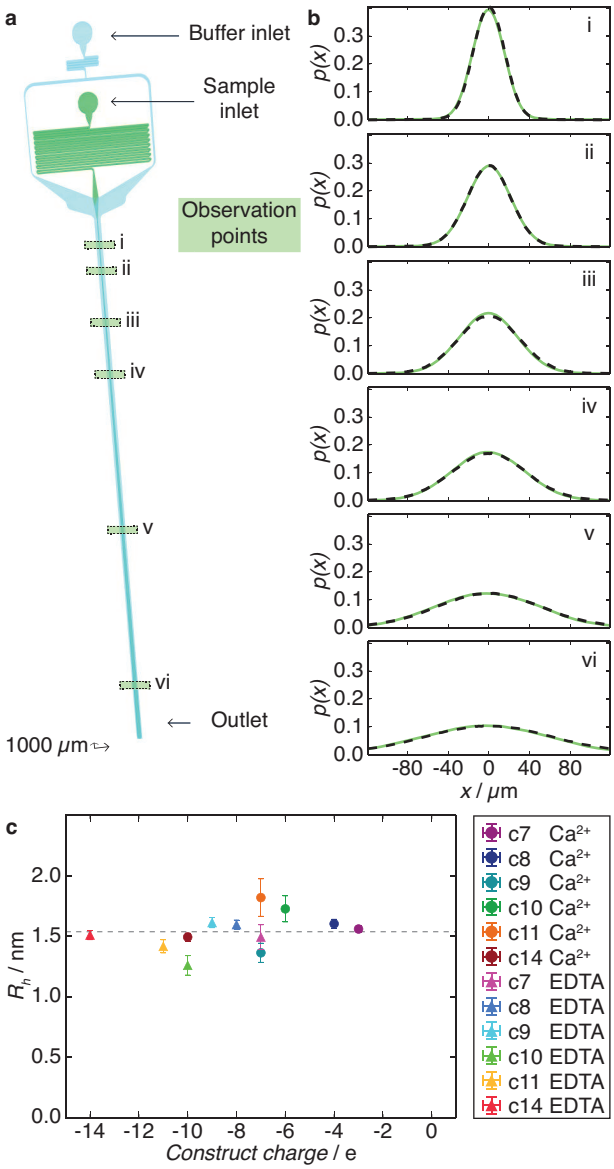

Fig. 3 Diffusion experiments. (a) Diagram of the microfluidic device used for the diffusion coefficient measurements showing the buffer and sample inlets and outlet. The 12 observation points are shaded in green. (b) The diffusion profiles of a calbindin sample, c9 in EDTA buffer, at every second of the 12 different incubation times. The solid green lines represent the data, and the dashed black lines show the fit. (c) Calculated radii for the 12 samples, the error bar shows the standard deviation between results from experiments at three flow rates: 80, 120 and 160 μLhr^{-1}. The dashed horizontal line indicates the mean radius of 1.5 ± 0.2 nm.

groups of all side chains would be expected to be predominantly in the protonated state.[31] However, pK_a perturbation of the N-terminus could still influence the charge of the folded proteins in solution. Furthermore, the different mutations introduced in each protein construct may not affect the overall charge equally. The change in the effective charge could depend on the specific electrostatic environment of each substitution, for instance in c11 the introduction of an aspartate residue in the already electronegative environment of the C-terminal EF-hand may have a reduced effect on the solvated charge compared to mutations elsewhere in the protein.[8]

The data shown in Fig. 4(a) indicate that there is a correlation between the expected charge of the primary protein structure plus any coordinated calcium ions and the measured effective charge of the solvated protein. Notably this does not appear to be a direct linear relationship. The measured charges of the protein constructs are smaller than the predicted sequence charges, likewise the variations between the solvated protein charges were smaller than the predicted range of dry charges. It is interesting to note that for the constructs predicted to carry a higher charge, the net charge appears to reach a plateau, Fig. 4(a). Qualitatively similar trends have been observed using capillary electrophoresis.[17] Crucially, we are able to capture this trend by investigating a large range of predicted construct charges.

To compare our results with qualitative data obtained through conventional methods, we investigated the constructs by native gel electrophoresis. Agarose gels were cast and run in buffer containing either 1 mM Ca^{2+} or 1 mM EDTA to probe the Ca^{2+} bound or apo form of the calbindin constructs, Fig. 4(c).[13]

3 Discussion

A significant fraction of residues, 27 out of 75 in wild type calbindin D_{9k} are expected to contain charged moieties at pH 8.[31–33] Detailed descriptions of the charges of colloid particles and surfaces with uniform charge distributions have been developed.[34,57] In particular, the empirical relationship between ζ and the surface charge at the Stern layer of a particle has been described by Loeb, Overbeek, and Wiersema.[34] The expression for this relationship predicts a plateau in the zeta potential as the surface charge increases and can be found in the electronic supplementary information†. Although the model for colloid particles cannot be applied directly to protein molecules with their heterogeneous distribution of opposing charges, the high charge density of the protein molecule could result in the observed non-linear relation between the effective and the construct charge, Fig. 4(a).

We investigated the specific effect of calbindin interaction with Ca^{2+} by characterising each construct in 5 mM Tris-HCl buffer containing either 0.1 mM $CaCl_2$ or EDTA. Through

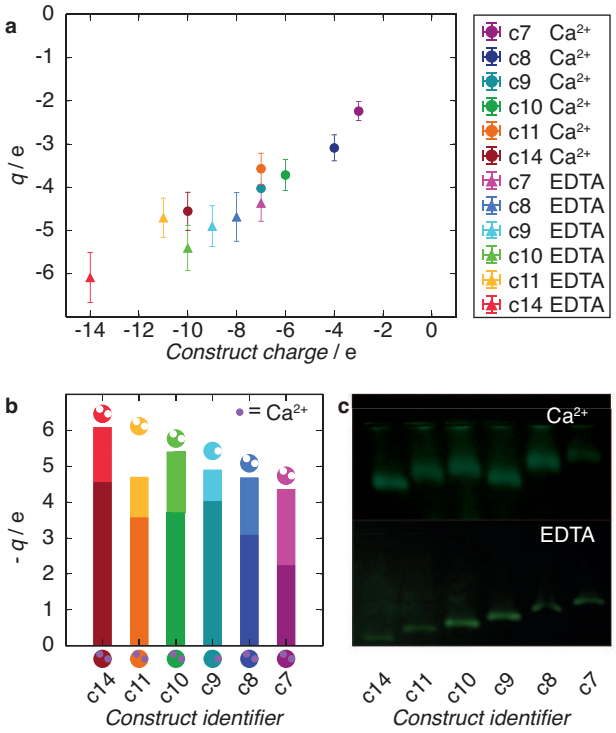

Fig. 4 Charge determination. (a) The net charges of the solvated calbindin constructs found by combining the measured electrophoretic mobilities with the mean diffusion coefficient. (b) The measured change in net charge as a result of the presence of free Ca^{2+}. The top and bottom of the bars correspond to the charge in the presence and absence of Ca^{2+} respectively. (c) Native gel electrophoresis of the six calbindin constructs in the presence of Ca^{2+} (top) or EDTA (bottom). The images show the fluorescence signal of the labelled constructs.

these experiments, we determined the change in the effective charge of calbindin caused by the interaction with Ca^{2+}, Fig. 4(b). This approach does not rely on specific knowledge of the dry construct charge. Thus, this strategy could be useful in probing the effect of specific solution parameters on solvated proteins.

Under the experimental conditions used here, all the calbindin constructs would be expected to chelate Ca^{2+}.[26,44–46] The change in the effective protein charge in the presence of Ca^{2+} is shown in Fig. 4(b). In all cases the addition of Ca^{2+} increased the effective protein charge. The construct with the disrupted EF-hand, c9, exhibited the smallest change in effective charge in the presence of calcium ions, this observation is in agreement with the binding of just one calcium ion. Construct c11, which corresponds to the deamidated form of E56, exhibited the second lowest change in effective charge in the presence of calcium, which could reflect a change in calcium binding affinity.

The observed increase in net charge was lower than the +2 e expected per chelated Ca^{2+}. Indeed, we measured a change in charge of up to +2 e for the binding of two calcium ions. It is possible that in the absence of Ca^{2+} calbindin is able to interact transiently with other ions present in the solution, the replacement of these counter ions by calcium ions would result in the observed change in the effective charge. The lesser effect on the protein net charge could furthermore be conferred by electrostatic interactions, such as intramolecular salt bridges and charge screening, either within the protein or by the electrolytes associated with the solvated macromolecule.

The relative migration of the protein constructs on the native gels was in qualitative agreement with our findings from free-flow electrophoresis, in that the relative positions of the protein bands on the gel did not correspond directly to the magnitudes of their expected relative charges, Fig. 4(c). For instance, c14 did not migrate twice as far as c7. As noted in the free-flow electrophoresis experiments, the mobility of c9 appeared to be less reduced than those of the other constructs in the presence of Ca^{2+}. Unlike the free-flow electrophoresis measurements, however, we could not directly compare the native gels run in the presence of Ca^{2+} or EDTA, as these reported on the relative movement through a matrix rather than providing a quantitative measurement of the absolute mobility.

In free-flow electrophoresis molecules are separated by the application of an electric field perpendicular to the direction of flow. Because the sample components are separated in a perpendicular direction to the fluid flow, rather than temporally in their arrival at a detector, free-flow electrophoresis has potential as both an analytical and a preparative method. Our adaptation of free-flow electrophoresis to the micrometer scale therefore confers a number of possible advantages. The volume and amount of sample material required for measurements within microfluidic channels are considerably lower

than those necessary for assays in bulk solution. The measurement time is reduced from minutes or hours to milliseconds and seconds. Given the device dimensions used in this study, electroosmotic flow does not have a significant influence on sample migration in the electric field.[37]

The sample position was monitored via a fluorescent label, this approach enabled the sample molecules to be visualised irrespective of their size. Unlike techniques relying on light scattering, where the light scattering properties scale with the analyte size, thus introducing a bias for the detection of larger species in a mixture. Within microfluidic channels it is possible to characterise sample molecules with dimensions from the ångström to the micrometer scale, a limit defined by the channel dimensions.

In this study we have used the fluorescence of a covalently attached fluorophore to visualise the sample molecules. This detection method has the advantage of enabling us to study electrostatic effects over a very wide range of protein concentrations. Low nM concentrations are routinely accessible with the appropriate optical equipment. With the method presented here it is therefore possible to investigate or alleviate by dilution concentration dependent electrostatic phenomena, such as screening at high protein concentrations.[2,31] However, although general labelling strategies are available, which can be applied to label for instance primary amines under native solution conditions, there is the risk of perturbing the protein structure or function through the introduction of a label. Future directions could therefore include exploring the intrinsic fluorescence of aromatic residues. Here, we found that the label did not alter the size of calbindin considerably.

4 Conclusions

In the present study we have presented an approach to quantify the effective charges of proteins under native conditions in free solution. We have used a microfluidic platform to determine both the electrophoretic mobility and the diffusion coefficient of a protein, and used the fluctuation-dissipation theorem to connect directly these measurements to the effective charge of the analyte without the requirement for any adjustable parameters or assumptions regarding the shape or size of the molecular species to be analysed. We have demonstrated that this method is applicable to analysing protein samples even at low micromolar concentrations, and have illustrated its applicability to characterise a charge-ladder family of mutants of the protein calbindin. These experiments shed light on the non-linear relation between construct charge and the effective charge of the solvated protein, providing insights into the fundamental physicochemical parameters characterising biomolecules in solution. Moreover, our findings demonstrate that microfluidic free-flow electrophoresis can detect non-covalent interactions, such as those between calbindin D_{9k} and Ca^{2+}. This method can therefore be applied to detect specific ion binding by proteins in solution. The methodology presented in this paper is generally applicable to investigate macromolecules in solution and can be applied to develop a quantitative framework of understanding for biomolecules and their non-covalent interactions in solution.

5 Acknowledgements

We would like to thank Dr Alex Buell for helpful discussions and Dr Jeremy Skepper (University of Cambridge) for assistance with the acquisition of the SEM images. Furthermore, we would like to acknowledge funding from the BBSRC (T.W.H., T.M. and T.P.J.K.), Marie Curie Actions (P.A.), the Newman Foundation and ERC (T.P.J.K.), and the Swedish Research Council (S.L.)

References

1 B. Honig and A. Nicholls, *Science*, 1995, **268**, 1144–1149.
2 S. Linse, B. Jönsson and W. J. Chazin, *Proc. Natl. Acad. Sci. U S A*, 1995, **92**, 4748–4752.
3 M. Lund and B. Jönsson, *Biochemistry*, 2005, **44**, 5722–5727.
4 B. Svensson, B. Jonsson, C. E. Woodward and S. Linse, *Biochemistry*, 1991, **30**, 5209–5217.
5 D. C. Bas, D. M. Rogers and J. H. Jensen, *Proteins*, 2008, **73**, 765–783.
6 M. H. M. Olsson, C. R. Søndergaard, M. Rostkowski and J. H. Jensen, *J. Chem. Theory Comput.*, 2011, **7**, 525–537.
7 S. Bietz, S. Urbaczek, B. Schulz and M. Rarey, *J. Cheminform.*, 2014, **6**, 12.
8 M. Lund and B. Jönsson, *Q. Rev. Biophys.*, 2013, **46**, 265–81.
9 N. D. Yilmazer and M. Korth, *J. Phys. Chem. B*, 2013, **117**, 8075–84.
10 R. Sure, J. Antony and S. Grimme, *J. Phys. Chem. B*, 2014, **118**, 3431–3440.
11 J. H. Jensen, *ArXiv*, 2015, 1–23.
12 K. Hannig, *Anal. Chem.*, 1961, **181**, 244–254.
13 B. G. Johansson, *Scand. J. Clin. Lab. Invest. Suppl.*, 1972, **29**, 7–19.
14 K. Hannig, H. Wirth, B. H. Meyer and K. Zeiller, *Hoppe-Seyler's Z. Physiol. Chem.*, 1975, **356**, 1209–1223.
15 J. Gao, F. A. Gomez, R. Härter and G. M. Whitesides, *Proc. Natl. Acad. Sci. U S A*, 1994, **91**, 12027–12030.
16 J. Gao and G. M. Whitesides, *Anal. Chem.*, 1997, **69**, 575–580.
17 J. D. Carbeck, I. J. Colton, J. Gao and G. M. Whitesides, *Acc. Chem. Res.*, 1998, **31**, 343–350.

18 R. Pecora, *J. Nanopart. Res.*, 2000, **2**, 123–131.

19 A. V. Delgado, F. González-Caballero, R. J. Hunter, L. K. Koopal and J. Lyklema, *Pure Appl. Chem.*, 2005, **77**, 1753–1805.

20 A. Lomakin, D. B. Teplow and G. B. Benedek, *Methods Mol. Biol.*, 2005, **299**, 153–174.

21 J. C. W. Corbett and R. O. Jack, *Colloids Surf. A*, 2011, **376**, 31–41.

22 A. L. Svensson, E. Thulin and S. Forsen, *J. Mol. Biol.*, 1992, 601–606.

23 C. S. Fullmer and R. H. Wasserman, *J. Biol. Chem.*, 1981, **256**, 5669–5674.

24 R. H. Kretsinger and C. E. Nockolds, *J. Biol. Chem.*, 1973, **248**, 3313–3326.

25 D. M. E. Szebenyi and K. Moffat, *J. Biol. Chem.*, 1986, **261**, 8761–8777.

26 S. Linse, P. Brodin, T. Drakenberg, E. Thulin, P. Sellers, K. Elmdén, T. Grundström and S. Forsén, *Biochemistry*, 1987, **26**, 6723–6735.

27 S. Christakos, *Rev. Endocr. Metab. Disord.*, 2012, **13**, 39–44.

28 J. Kördel, N. J. Skelton, M. Akke and W. J. Chazin, *J. Mol. Biol.*, 1993, **231**, 711–734.

29 N. J. Skelton, J. Kordel, M. Akke, S. Forsén and W. J. Chazin, *Nat Struct Mol Biol*, 1994, **1**, 239–245.

30 B. Wendt, T. Hofmann, S. R. Martin, P. Bayley, P. Brodin, T. Grundström, E. Thulin, S. Linse and S. Forsén, *FEBS J.*, 1988, **175**, 439–445.

31 T. Kesvatera, B. Jönsson, E. Thulin and S. Linse, *J. Mol. Biol.*, 1996, **259**, 828–839.

32 T. Kesvatera, B. Jönsson, E. Thulin and S. Linse, *Proteins*, 2001, **45**, 129–35.

33 T. Kesvatera, B. Jönsson, A. Telling, V. Tõugu, H. Vija, E. Thulin and S. Linse, *Biochemistry*, 2001, **40**, 15334–40.

34 R. J. Hunter, *Zeta Potential in Colloid Science: Principles and Applications*, Academic Press, New York and London, 1981.

35 D. Kohlheyer, G. A. J. Besselink, S. Schlautmann and R. B. M. Schasfoort, *Lab. Chip.*, 2006, **6**, 374–380.

36 A. C. Siegel, D. A. Bruzewicz, D. B. Weibel and G. M. Whitesides, *Adv. Mater.*, 2007, **19**, 727–733.

37 D. Kohlheyer, J. C. T. Eijkel, A. van den Berg and R. B. M. Schasfoort, *Electrophoresis*, 2008, **29**, 977–993.

38 W. Ebina, A. C. Rowat and D. a. Weitz, *Biomicrofluidics*, 2009, **3**, 34104.

39 A. R. Abate, T. Hung, P. Mary, J. J. Agresti and D. A. Weitz, *Proc. Natl. Acad. Sci. U S A*, 2010, **107**, 19163–19166.

40 S. Köhler, C. Weilbeer, S. Howitz, H. Becker, V. Beushausen and D. Belder, *Lab. Chip.*, 2011, **11**, 309–314.

41 J.-H. So and M. D. Dickey, *Lab. Chip.*, 2011, **11**, 905–911.

42 Y. Song, Z. Liu, T. Kong and H. C. Shum, *Chem. Commun.*, 2013, **49**, 1726–8.

43 T. W. Herling, T. Müller, L. Rajah, J. N. Skepper, M. Vendruscolo and T. P. J. Knowles, *Appl. Phys. Lett.*, 2013, **102**, 184102.

44 S. Linse, P. Brodin, C. Johansson, E. Thulin, T. Grundström and S. Forsén, *Nature*, 1988, **335**, 651–652.

45 D. Dell'Orco, W.-F. Xue, E. Thulin and S. Linse, *Biophys. J.*, 2005, **88**, 1991–2002.

46 I. André and S. Linse, *Anal. Biochem.*, 2002, **305**, 195–205.

47 N. Panchuk-Voloshina, R. P. Haugland, J. Bishop-Stewart, M. K. Bhalgat, P. J. Millard, F. Mao and W. Y. Leung, *J. Histochem. Cytochem.*, 1999, **47**, 1179–1188.

48 M. Akke and S. Forsén, *Proteins*, 1990, **8**, 23–29.

49 K. Beckingham, *J. Biol. Chem.*, 1991, **266**, 6027–6030.

50 P. Brodin, C. Johansson, S. Forsén, T. Drakenberg and T. Grundström, *J. Biol. Chem.*, 1990, **265**, 11125–11130.

51 S. Linse, C. Johansson, P. Brodin, T. Grundström, T. Drakenberg and S. Forsén, *Biochemistry*, 1991, **30**, 154–162.

52 A. E. Kamholz, B. H. Weigl, B. A. Finlayson and P. Yager, *Anal. Chem.*, 1999, **71**, 5340–5347.

53 A. Hatch, A. E. Kamholz, K. R. Hawkins, M. S. Munson, E. A. Schilling, B. H. Weigl and P. Yager, *Nat. Biotech.*, 2001, **19**, 461–465.

54 a. E. Kamholz, E. a. Schilling and P. Yager, *Biophys. J.*, 2001, **80**, 1967–1972.

55 C. T. Culbertson, S. C. Jacobson and J. Michael Ramsey, *Talanta*, 2002, **56**, 365–373.

56 S. Achuthan, B. J. Chung, P. Ghosh, V. Rangachari and A. Vaidya, *BMC Bioinform.*, 2011, **12**, S13.

57 J. Delgado, A, Gonzalez-Caballero, F, Bruque, *J. Colloid Interf. Sci.*, 1986, **113**, 203–211.